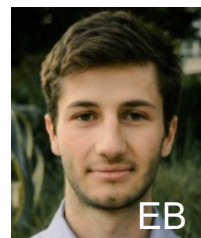
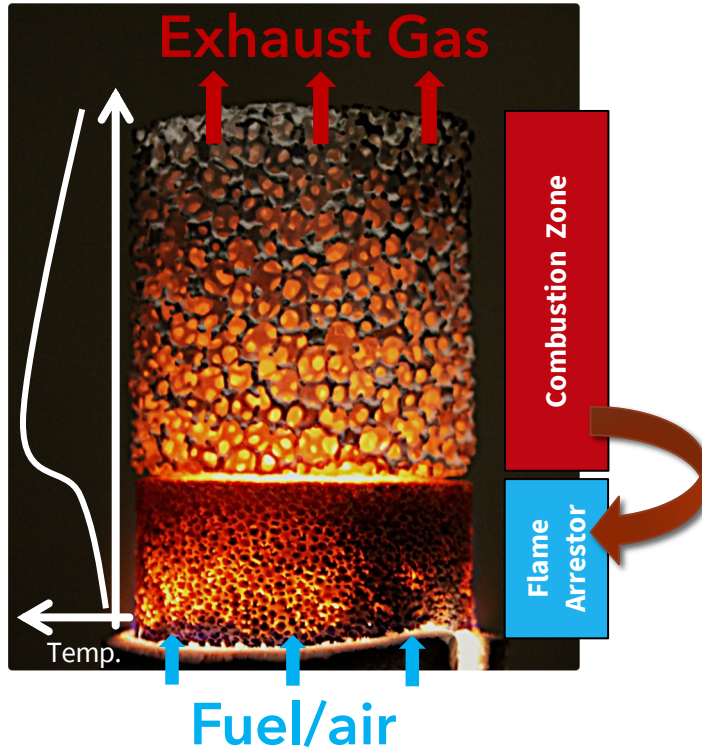


Ammonia combustion in inert porous media burners: systematic experimental characterization and chemical kinetics analysis

G.Vignat, T. Zirwes, E. R. Toro, E. Boigné, D. Trimis, M. Ihme



Porous media combustion



Applications in:

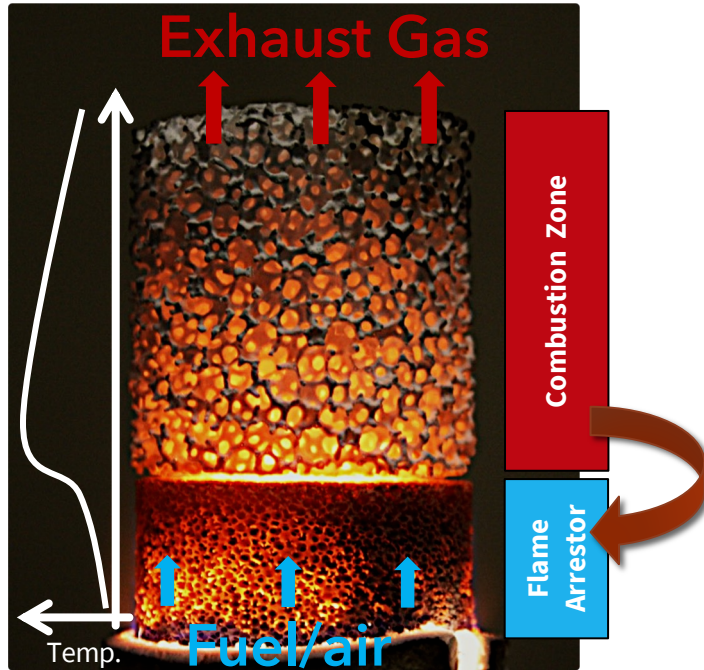
- Gas turbines
- Domestic boilers
- Radiant industrial heaters

Heat recirculation through solid matrix:

- Pre-heats fresh reactants
- Increases the flame speed

Ellzey et al., *Prog. Energy Combust. Sci.* 72 (2019).
 Wood and Harris, *Prog. Energy Combust. Sci.* 34 (2008).
 Trimis and Durst, *Combust. Sci. Technol.* 121 (1996).
 Sobhani et al., *Proc. Combust. Inst.* 37(4) (2019).

Porous media combustion



Key concept: Internal Heat recirculation by heat-conducting solid-ceramic matrix

Extended power modulation

Low noise emission

Reduction in CO, NO, unburnt fuel

Fuel-flexible operation

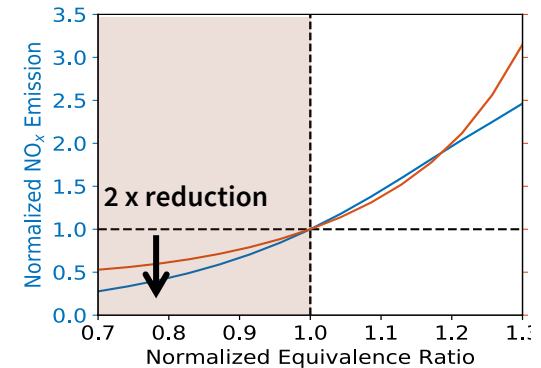
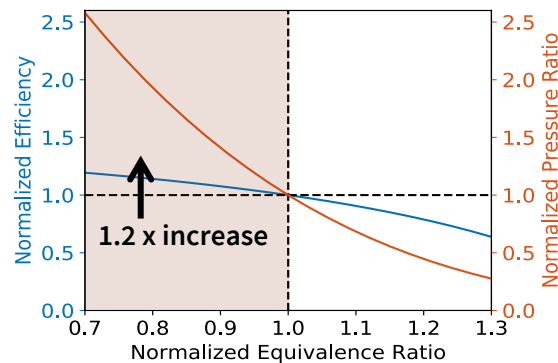
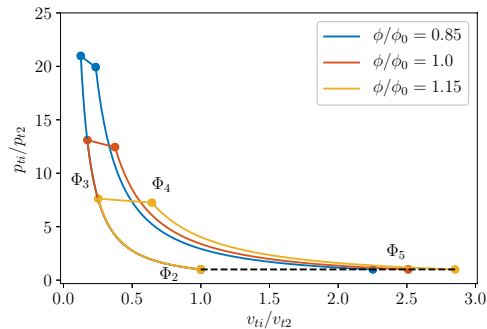
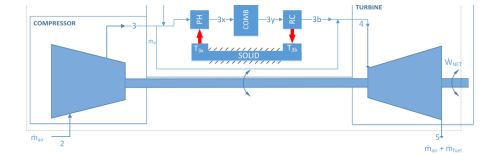
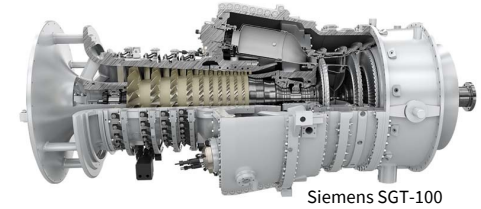
Combustion of ultra-lean fuel/air mixtures

No thermo-acoustic instabilities

Benefits of porous media combustion

Thermodynamic cycle analysis

- Replace primary combustion zone with PMC
- Extended lean flammability limit
 - ➔ Increase compression ratio
 - ➔ increase thermal efficiency by 20%
 - ➔ reduce emissions of NO_x by 50%



Why PMBs for ammonia?

Heat recirculation through solid matrix [2,3]:

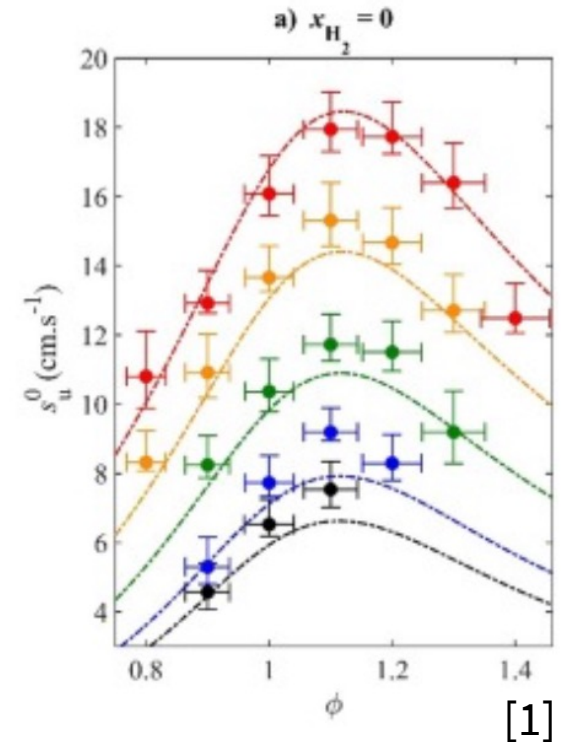
- Pre-heats fresh reactants
- **Increases the flame speed**
- **Enables very lean/rich combustion**
 - › Reduced pollutant emissions
 - › Improved thermodynamic efficiency [4]

[1] Lhuillier et al., *Fuel* 263 (2021).

[2] Ellzey et al., *Prog. Energy Combust. Sci.* 72 (2019).

[3] Masset et al., *Combust. Theory Model.* 25 (2021).

[4] Mohaddes et al., *Energy* 207 (2020).

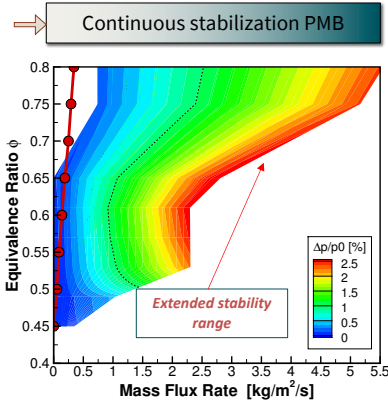
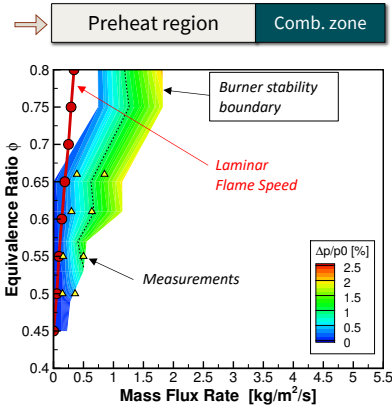
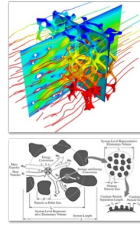


T_u			
●	298 K Present work	★	298 K Ichikawa
●	323 K Present work	▲	298 K Han
●	373 K Present work	◆	298 K Lee
●	423 K Present work	■	293 K Li
●	473 K Present work		

Why PMBs for ammonia?

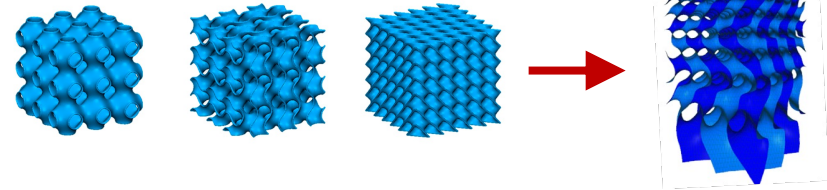
Computational design optimization

$$\begin{aligned} \text{Mass conservation: } & \frac{\partial(\rho_g \epsilon)}{\partial t} + \frac{\partial(\rho_g u \epsilon)}{\partial x} = 0 \\ \text{Species conservation: } & \rho_g \epsilon \frac{\partial Y_i}{\partial t} + \rho_g \epsilon u \frac{\partial Y_i}{\partial x} + \frac{\partial}{\partial x} (\rho_g \epsilon Y_i V_i) - \dot{\omega} W_i \epsilon = 0 \\ \text{Energy conservation: } & \rho_g \epsilon C_p \frac{\partial T_g}{\partial t} + \rho_g \epsilon C_p u \frac{\partial T_g}{\partial x} + \epsilon \sum_{i=1}^n \rho_{g,i} C_{p,i} V_i Y_i \frac{\partial T_g}{\partial x} + \epsilon \sum_{i=1}^n \dot{\omega}_i h_i W_i - \frac{\partial}{\partial x} (k_{g,e,f} \epsilon \frac{\partial T_g}{\partial x}) + h_v (T_g - T_s) = 0 \\ \text{Solid temperature: } & \rho_s C_s \frac{\partial T_s}{\partial t} + \frac{\partial}{\partial x} (\lambda_s \frac{\partial T_s}{\partial x}) + \frac{dq}{dx} - h_v (T_g - T_s) = 0 \end{aligned}$$

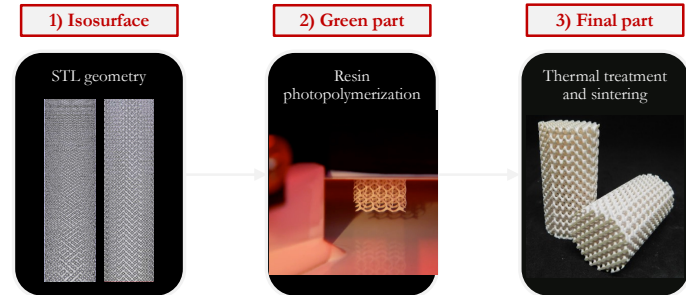


Tailoring porous-ceramic foams

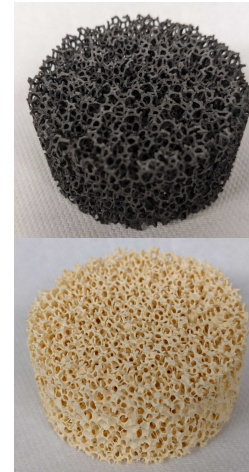
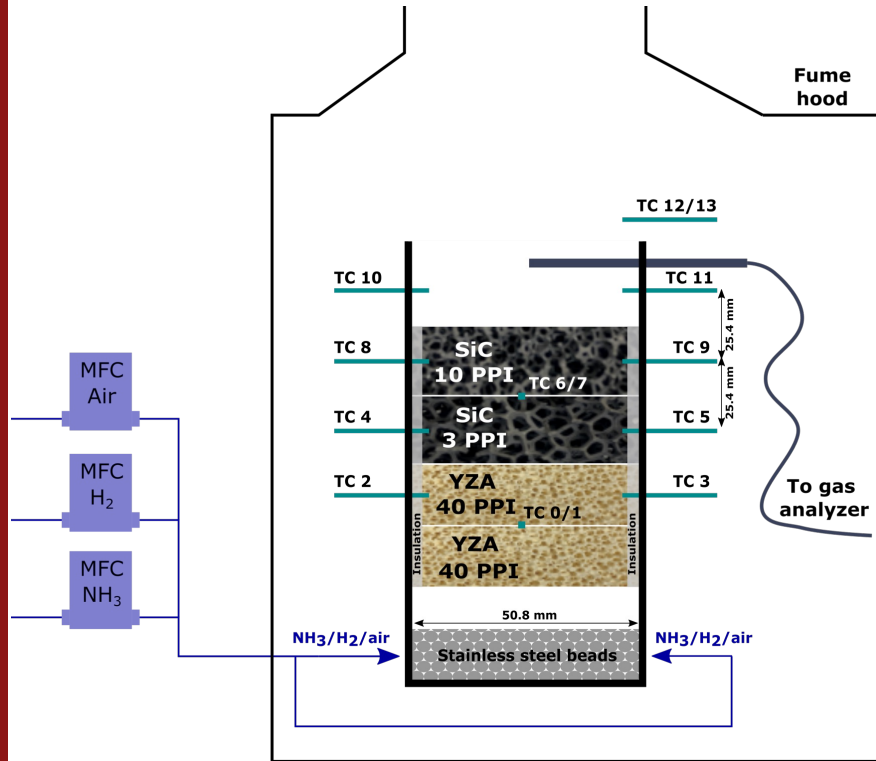
Triply-periodic minimal surfaces: control of topology and material properties



Additive Manufacturing Ceramics

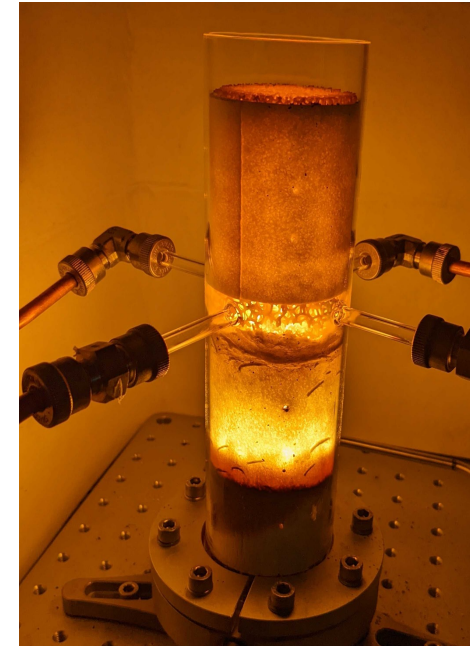


Experimental setup: Interface stabilized PMB

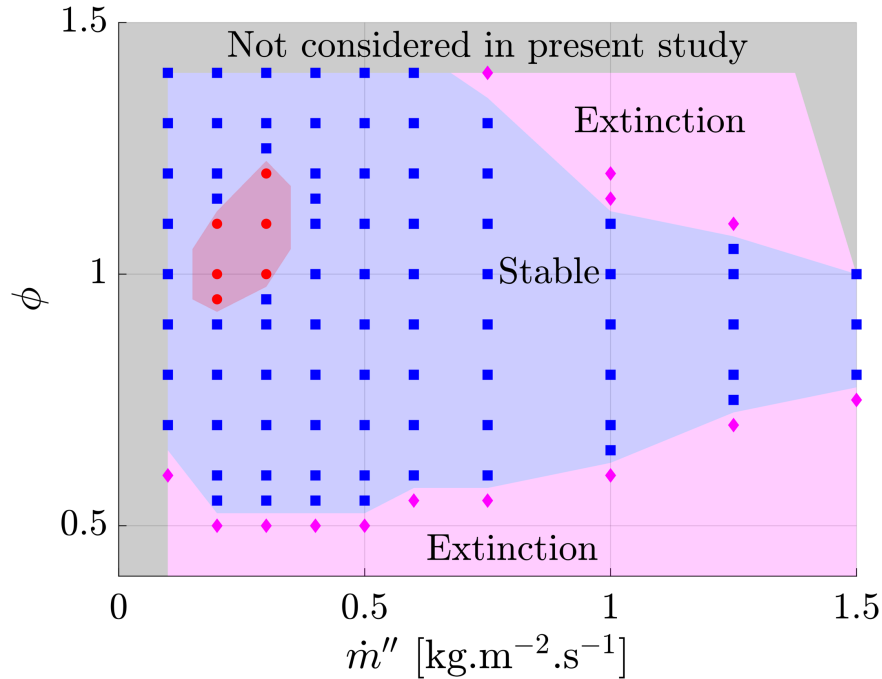


Combustion
Heat
recirculation

Flame
Arrestor

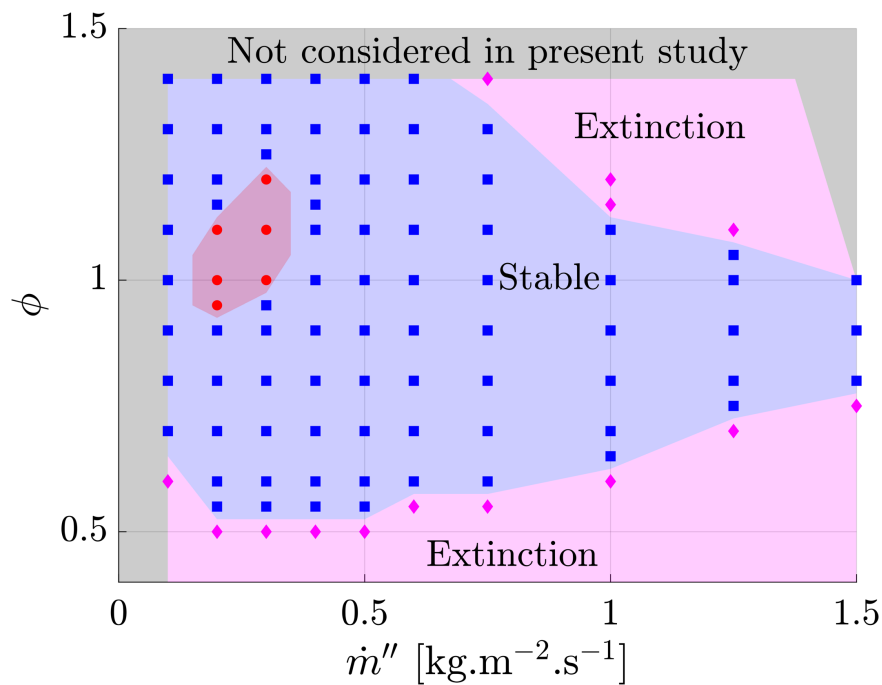


Extended flame stabilization

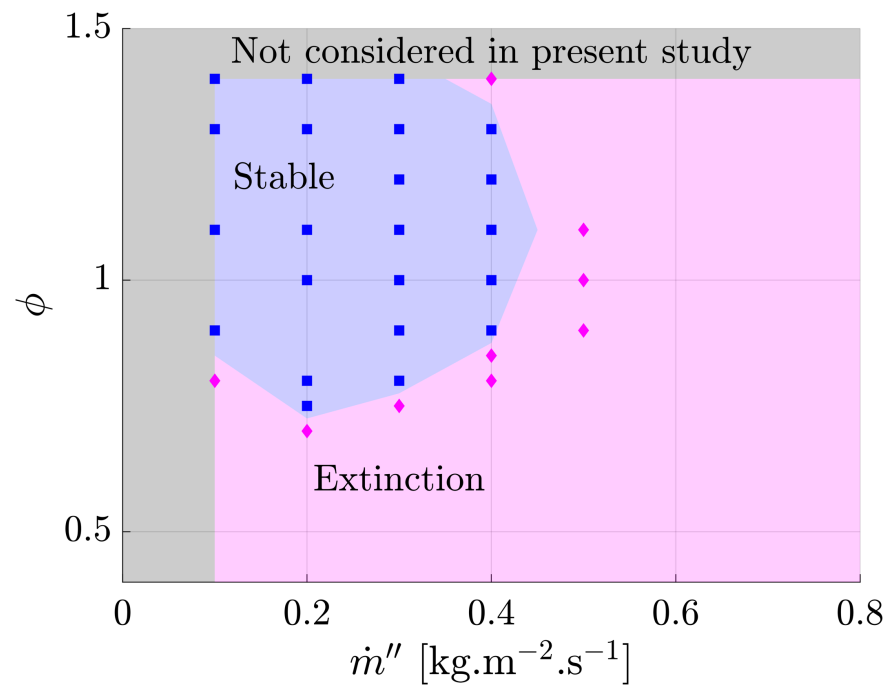


- Results for a $x_{NH_3} = 0.7$, $x_{H_2} = 0.3$ mixture
- Extended stability region, from:
 - Lean: $\phi_{LBO} = 0.55$
 - To rich conditions: $\phi = 1.4$
- Turndown ratio greater than 15:1
- Power density up to 62 MW.m⁻³
 - Estimated 5 to 24 MW.m⁻³ for swirl flames at atmospheric pressure

Extended flame stabilization: pure NH₃ operation



$$x_{NH_3} = 0.7, x_{H_2} = 0.3$$

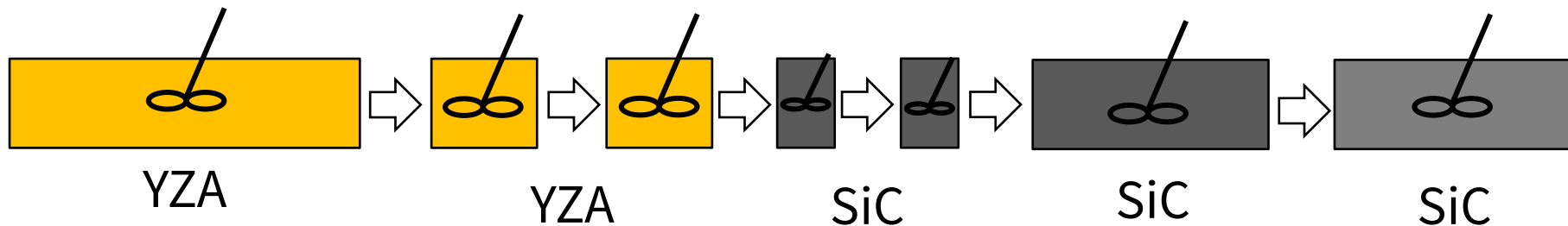


$$x_{NH_3} = 1$$

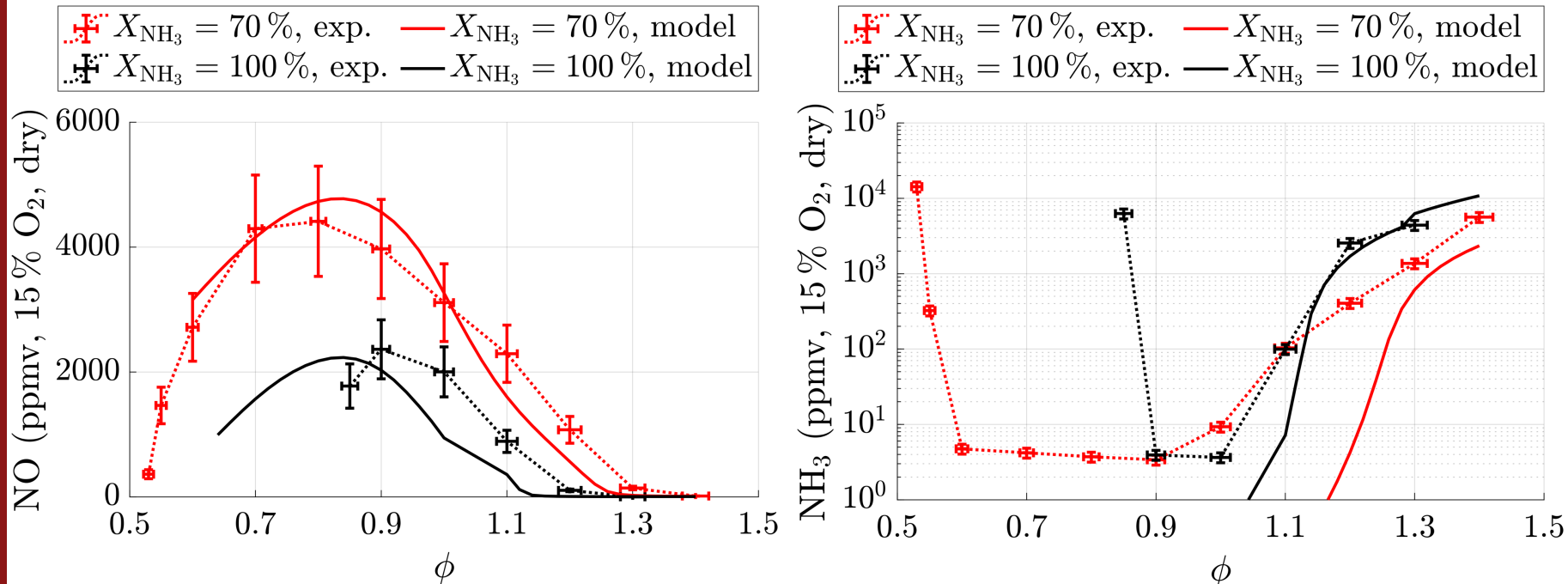
0D reactor network for PMB

7 continuously stirred **reactor network model** extended with **interphase** (solid-gas) heat transfer

- Reaction mechanism by Stagni et al., *Reac Chem Eng* 5(4), 2020.
- Interphase heat transfer (Bedoya et al., *Combust Flame* 162, 2015)
- **Effective material properties computed from x-ray tomographies**
- Inter-reactor heat transfer including radiation and conduction

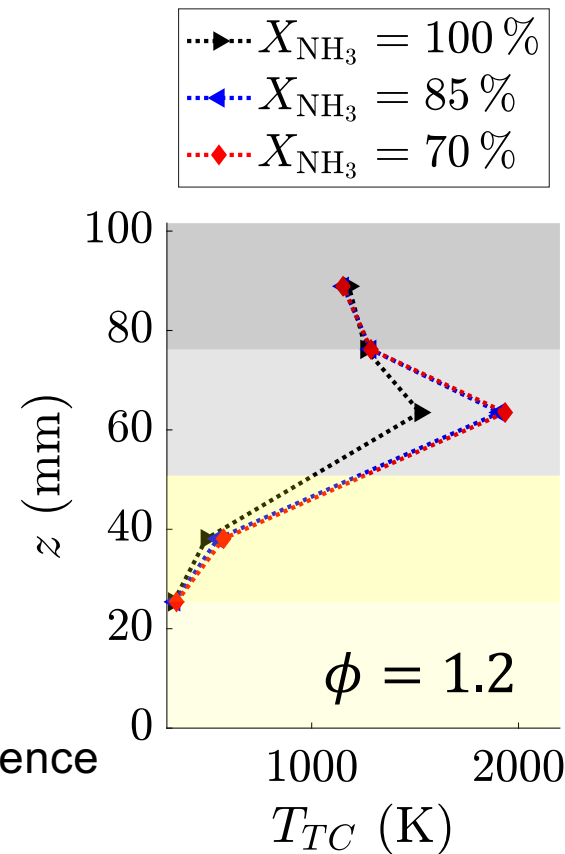
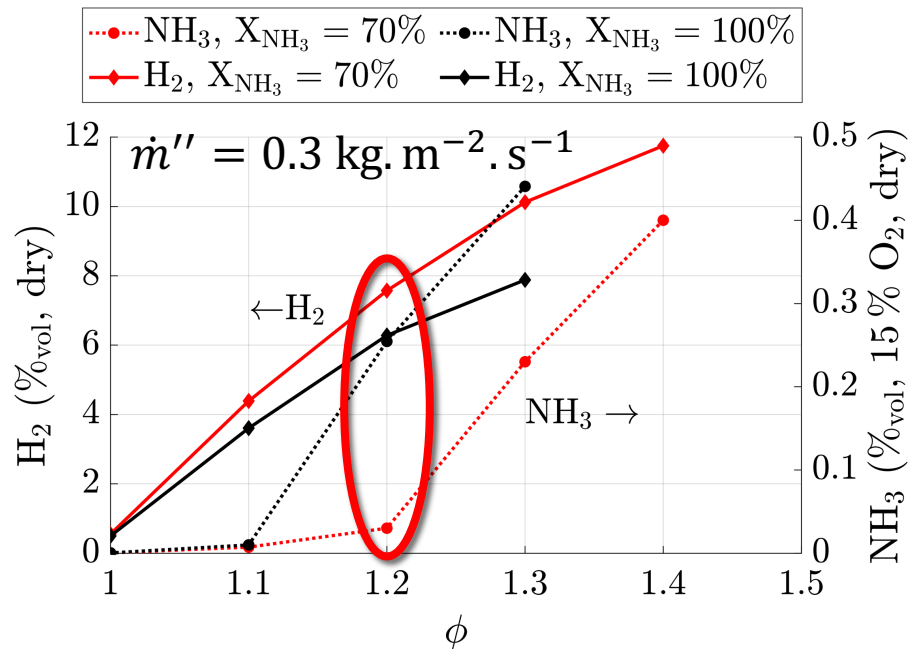


Burner pollutant emissions and model validation



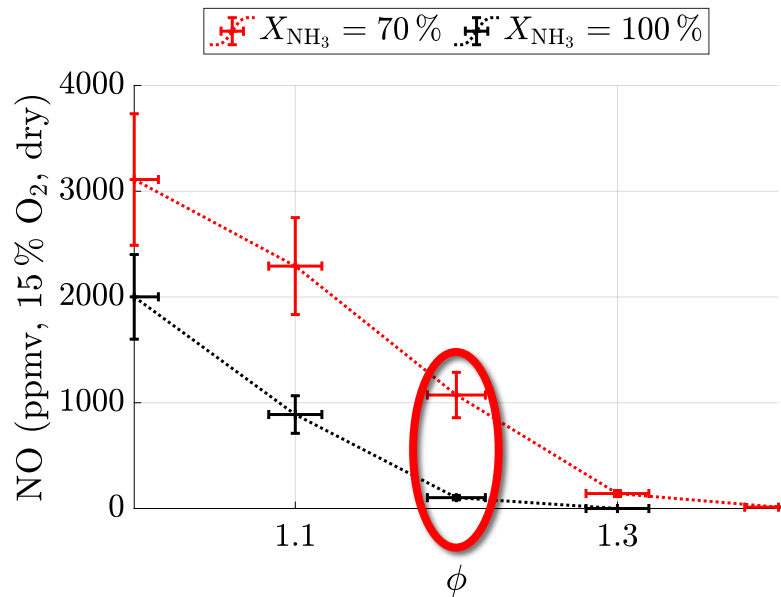
- Results for $\dot{m}'' = 0.3 \text{ kg} \cdot \text{m}^{-2} \cdot \text{s}^{-1}$
- The reactor network model captures NO emissions to good accuracy.
- Model breaks for weakly stabilized flames in the very lean region.

Exhaust composition in the rich regime: H₂/NH₃ ratio

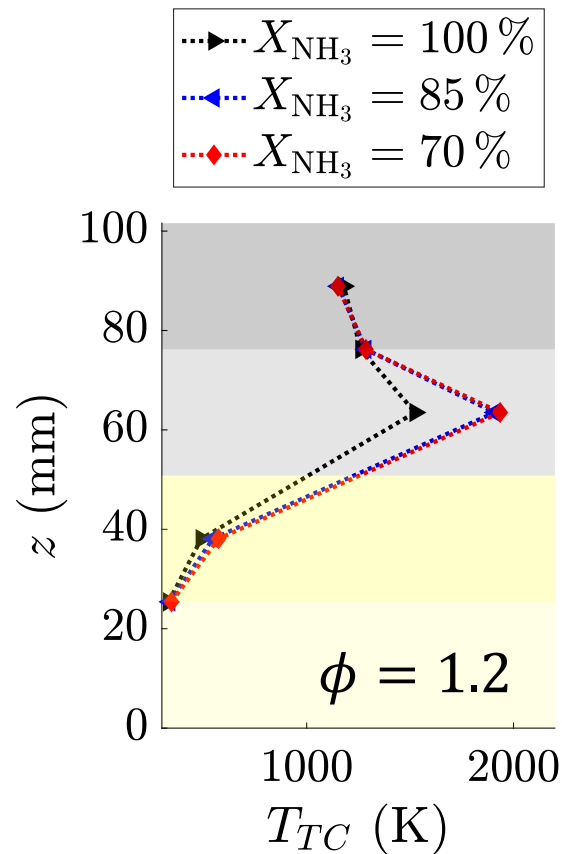


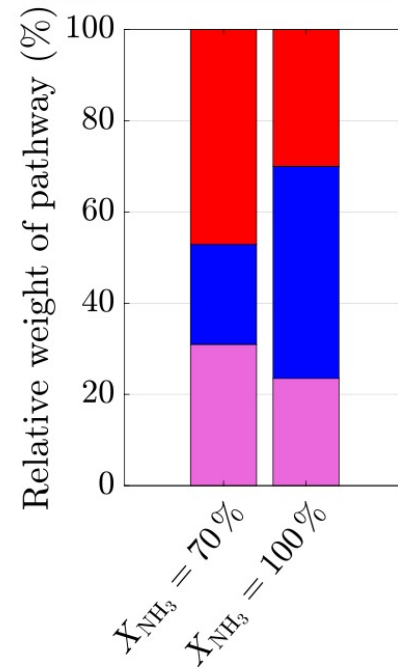
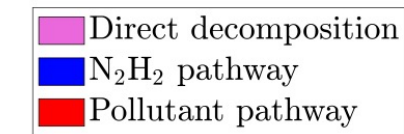
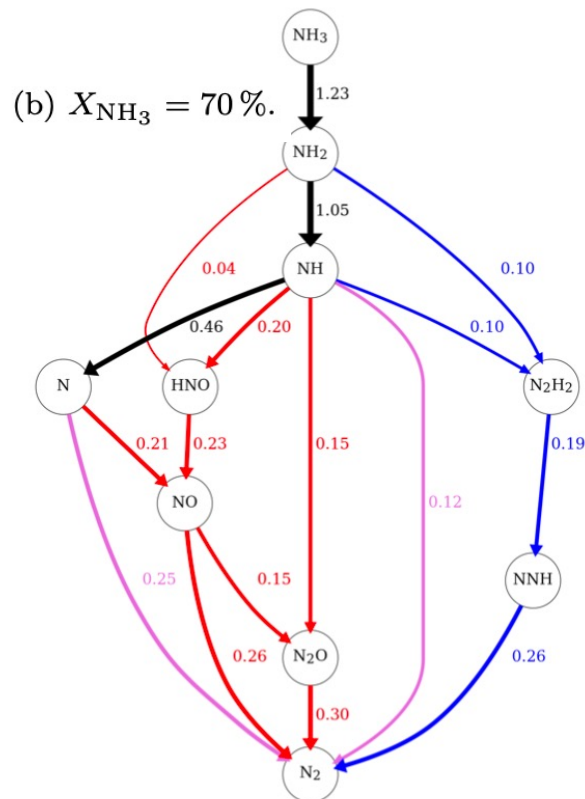
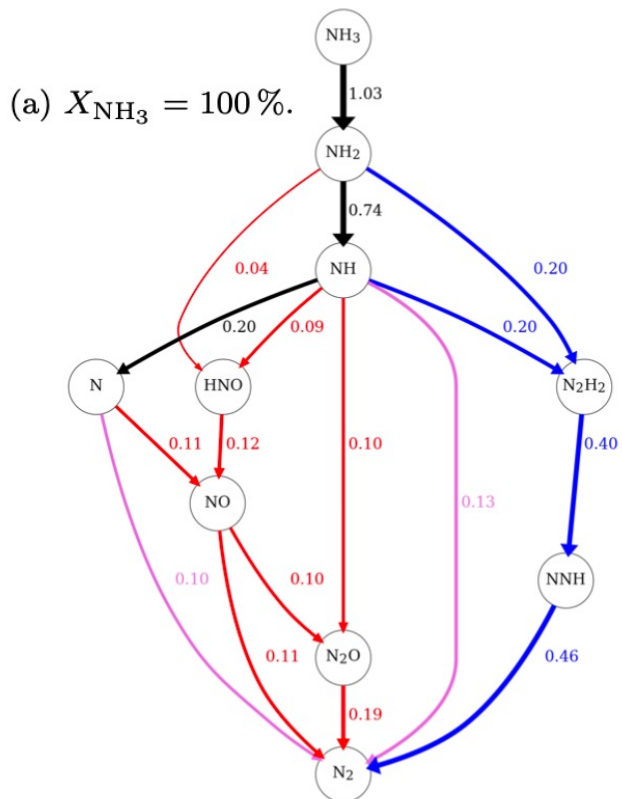
- High conversion of NH₃ to H₂ in rich conditions
- $\phi = 1.2$: a ~ 100 K difference in burner temperature explains the lower consumption rate of NH₃ and presence of unburnt in the exhaust stream (reactor network)

Exhaust composition in the rich regime: NO emissions



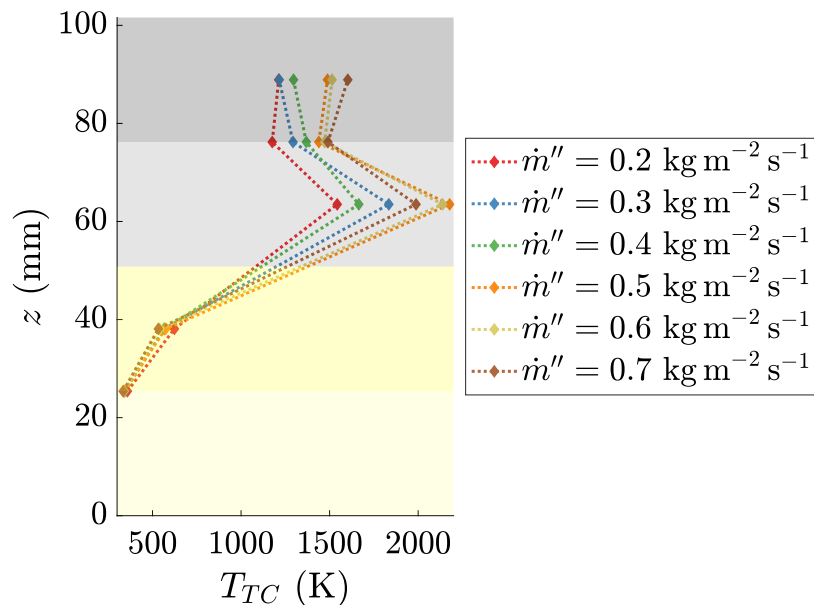
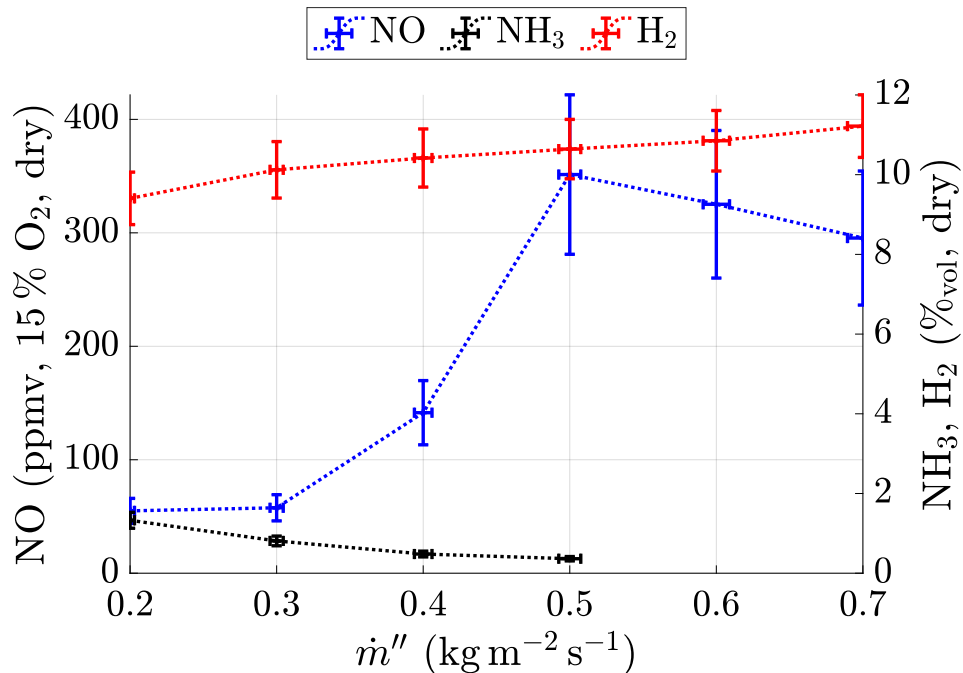
- Constant mass flux: $\dot{m}'' = 0.3 \text{ kg} \cdot \text{m}^{-2} \cdot \text{s}^{-1}$
- Fast decrease of NO emissions with increasing ϕ
- Emissions systematically lower for pure NH₃





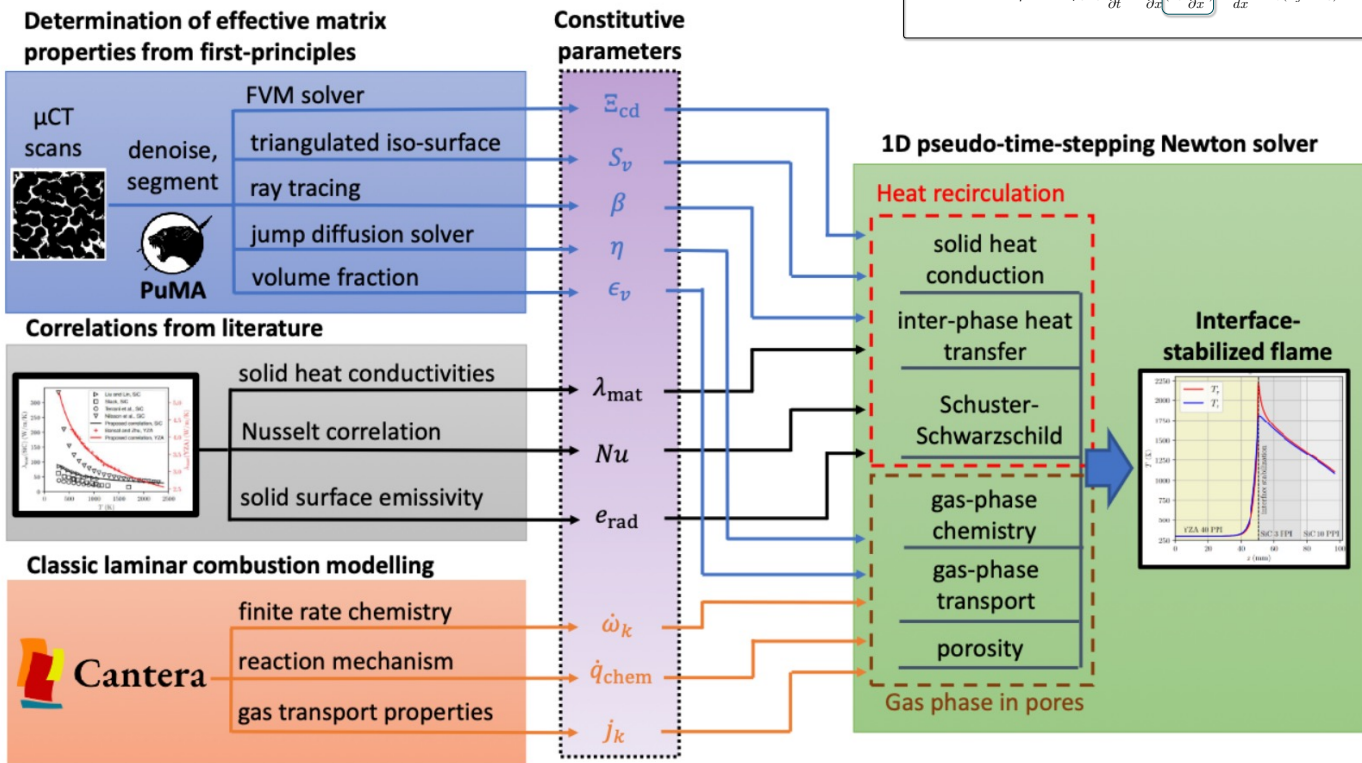
- 2 factors combine to explain lower NO emissions for the X_{NH_3} :
 - Lower NO formation rates in the flame region
 - Unburnt NH_3 and NH_2 in the post-flame region

Emissions at rich conditions: effect of mass flux



- Mass flux has a small influence on pollutant emission
- Increasing reforming efficiency with increasing mass flux
- Increasing NO emissions correlated with increasing operating temperatures

1D simulation framework



$$\text{Mass conservation: } \frac{\partial(\rho_g \epsilon)}{\partial t} + \frac{\partial(\rho_g u \epsilon)}{\partial x} = 0$$

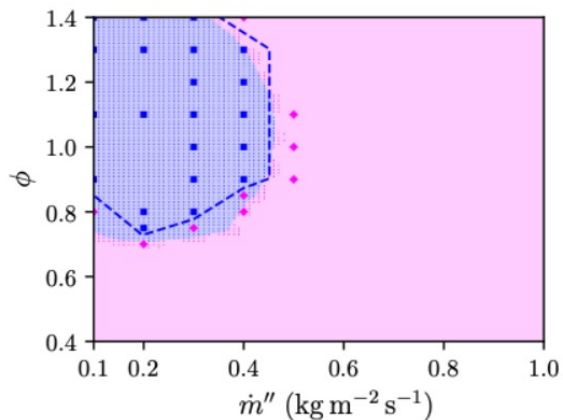
$$\text{Species conservation: } \rho_g \epsilon \frac{\partial Y_i}{\partial t} + \rho_g \epsilon u \frac{\partial Y_i}{\partial x} + \frac{\partial}{\partial x} (\rho_g \epsilon Y_i V_i) - \dot{\omega} W_i \epsilon = 0$$

$$\text{Energy conservation: } \rho_g \epsilon C_g \frac{\partial T_g}{\partial t} + \rho_g \epsilon C_g u \frac{\partial T_g}{\partial x} + \epsilon \sum_{i=1}^n \rho_{g,i} C_{g,i} V_i Y_i \frac{\partial T_g}{\partial x} + \epsilon \sum_{i=1}^n \dot{\omega}_i h_i W_i - \frac{\partial}{\partial x} (k_{g,\epsilon} \epsilon \frac{\partial T_g}{\partial x}) + h_v (T_g - T_s) = 0$$

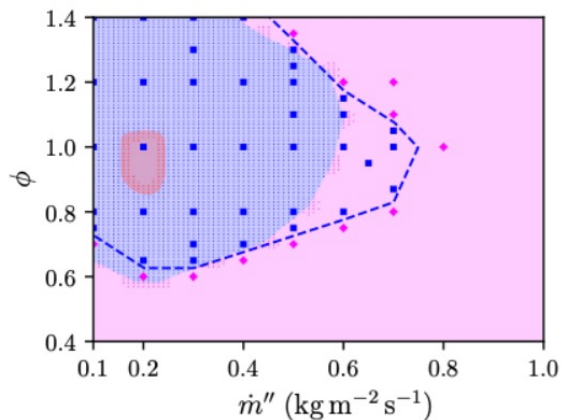
$$\text{Solid temperature: } \rho_s C_s \frac{\partial T_s}{\partial t} + \frac{\partial}{\partial x} (\lambda_s \frac{\partial T_s}{\partial x}) + \frac{dq}{dx} - h_v (T_g - T_s) = 0$$

1D simulation framework

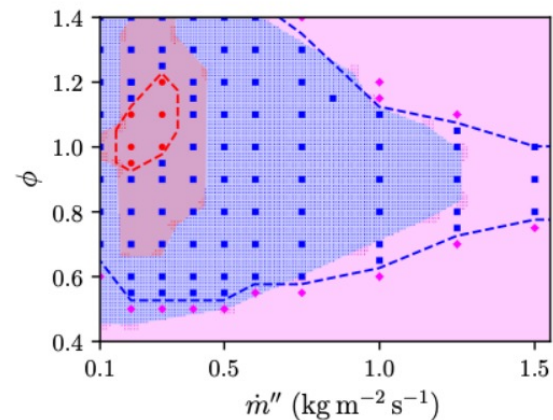
Simulations conducted using the 1D-VAS-FP framework (Table 5 and Sections 3 and 4.1).



(a) $X_{\text{NH}_3} = 100\%$



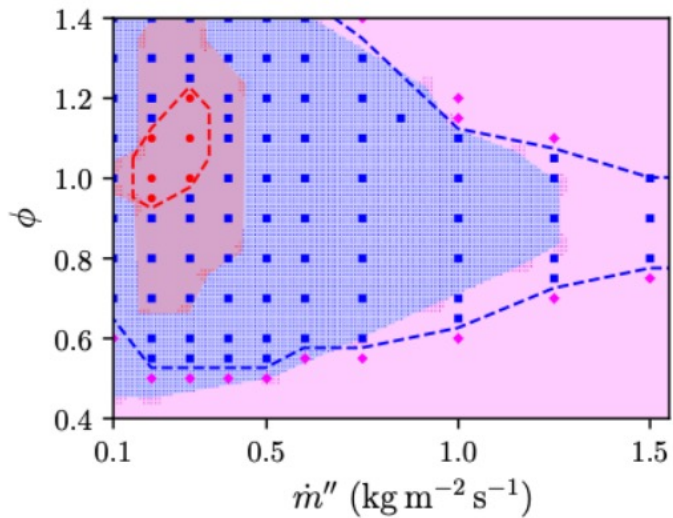
(b) $X_{\text{NH}_3} = 85\%$



(c) $X_{\text{NH}_3} = 70\%$

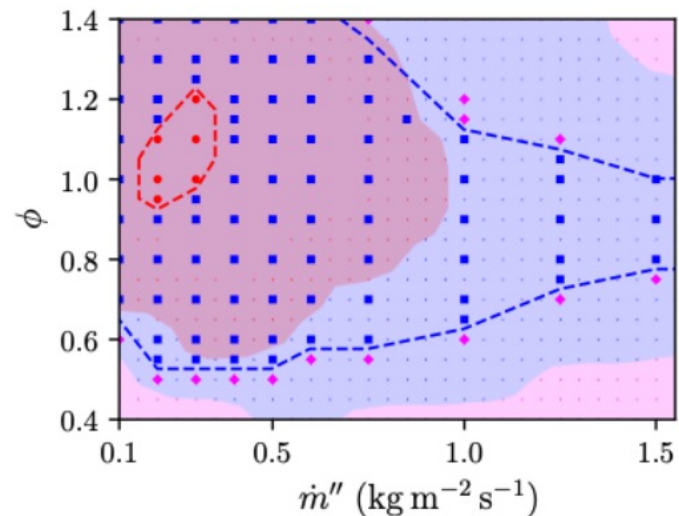
- 1D simulations can capture the experimentally determined stability limits of the burner when accurate constitutive relations are used.
- Pollutant emissions are also captured well.

1D simulation framework



(c) $X_{\text{NH}_3} = 70\%$

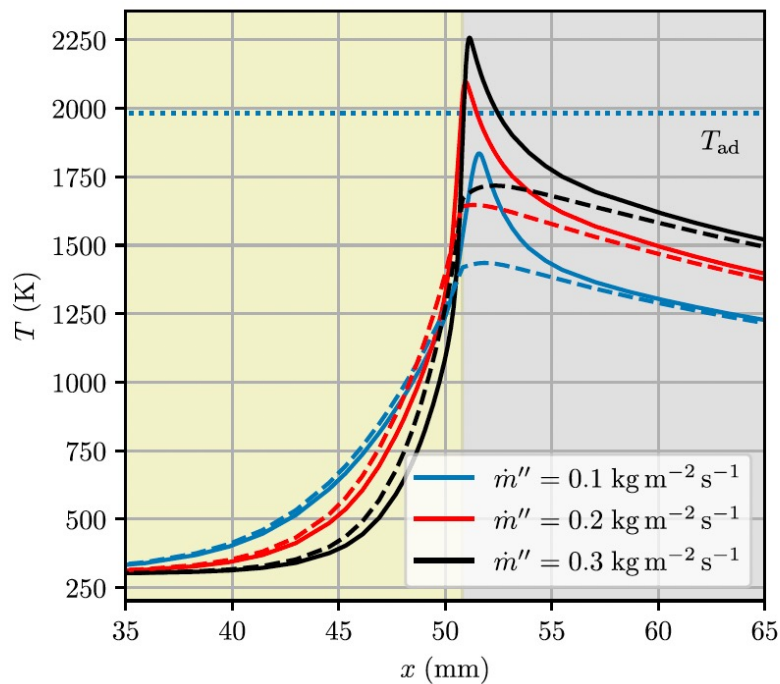
Accurate constitutive relations
from processed μ CT scans.



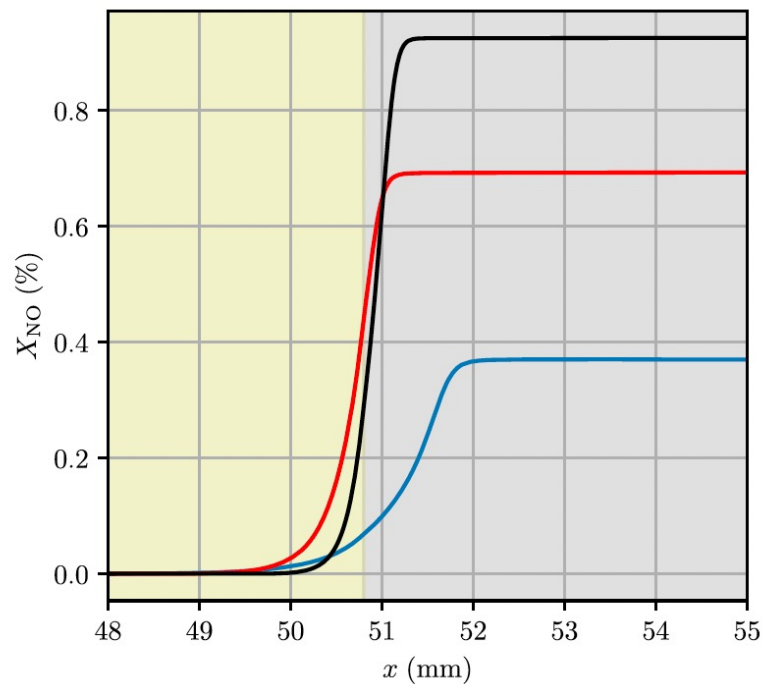
(f) $X_{\text{NH}_3} = 70\%$

Literature correlations for
constitutive relations.

1D Simulations

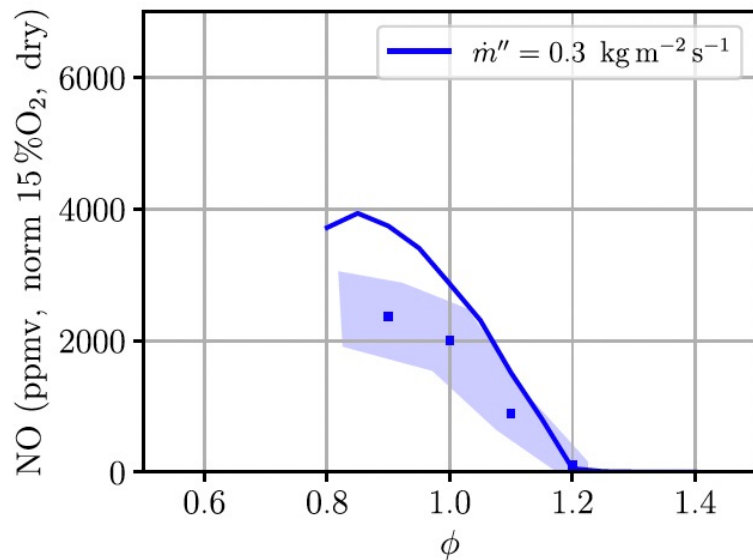
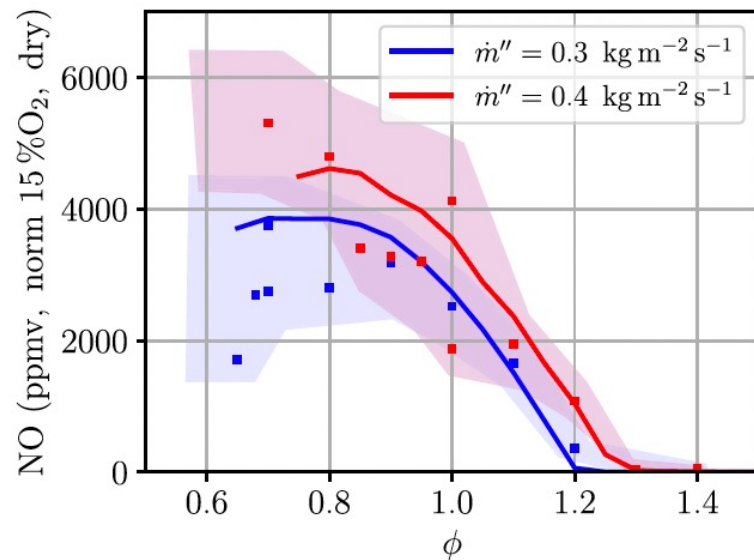


(a) Temperature



(b) NO mole fraction

1D Simulations

(a) $X_{\text{NH}_3} = 100\%$ (b) $X_{\text{NH}_3} = 85\%$

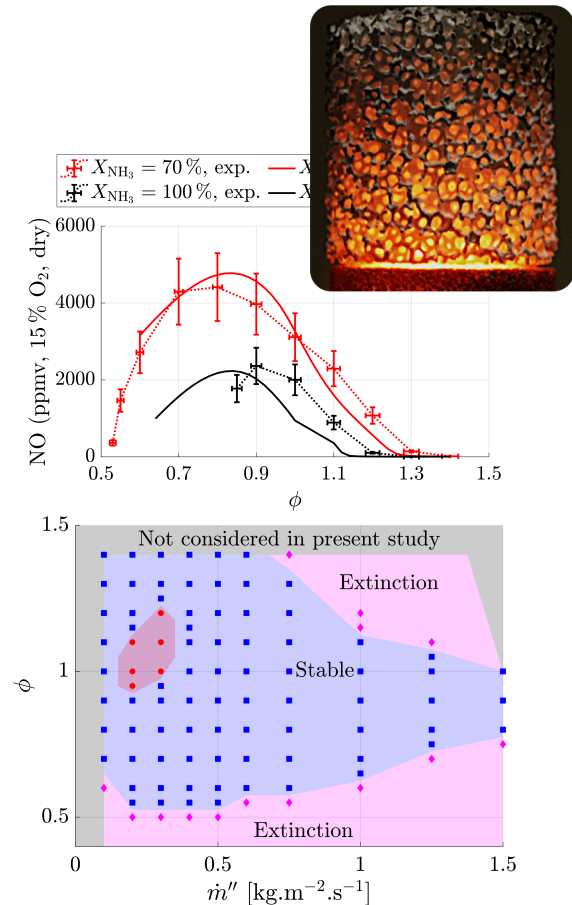
Conclusions

Demonstrated first **porous media burner for pure NH₃ combustion.**

Characterized NO, NH₃ and H₂ emissions:

- › In rich condition: most unburnt gases in the form of unburnt H₂
- › Unburnt NH₃ highly dependent on burner operating temperature

Introduced a reactor network and a 1D model with interphase heat transfer that captures emissions and stability to acceptable accuracy



References

- G Vignat, B Akoush, ER Toro, E Boigné, M Ihme, Combustion of lean ammonia-hydrogen fuel blends in a porous media burner, **Proceedings of the Combustion Institute** 39 (4), 4195-4204, 2023.
- T Zirwes, G Vignat, ER Toro, E Boigné, K Younes, D Trimis, M Ihme, Improving volume-averaged simulations of matrix-stabilized combustion through direct X-ray μ CT characterization: Application to NH₃/H₂-air combustion, **Combustion and Flame** 257, 113020, 2023.
- G Vignat, T Zirwes, ER Toro, K Younes, E Boigné, P Muhunthan, L Simitz, D Trimis, M Ihme, Experimental and numerical investigation of flame stabilization and pollutant formation in matrix stabilized ammonia-hydrogen combustion, **Combustion and Flame** 250, 112642, 2023.
- D Mohaddes, C Chang, M Ihme, Thermodynamic cycle analysis of superadiabatic matrix-stabilized combustion for gas turbine engines, **Energy** 207, 118171, 2020.
- S Sobhani, D Mohaddes, E Boigne, P Muhunthan, M Ihme, Modulation of heat transfer for extended flame stabilization in porous media burners via topology gradation, **Proceedings of the Combustion Institute** 37 (4), 5697-5704, 2019.
- S Sobhani, S Allan, P Muhunthan, E Boigne, M Ihme, Additive Manufacturing of Tailored Macroporous Ceramic Structures for High-Temperature Applications, **Advanced Engineering Materials** 22 (8), 2000158, 2020.